HNPS Advances in Nuclear Physics

Vol 19 (2011)

HNPS2011

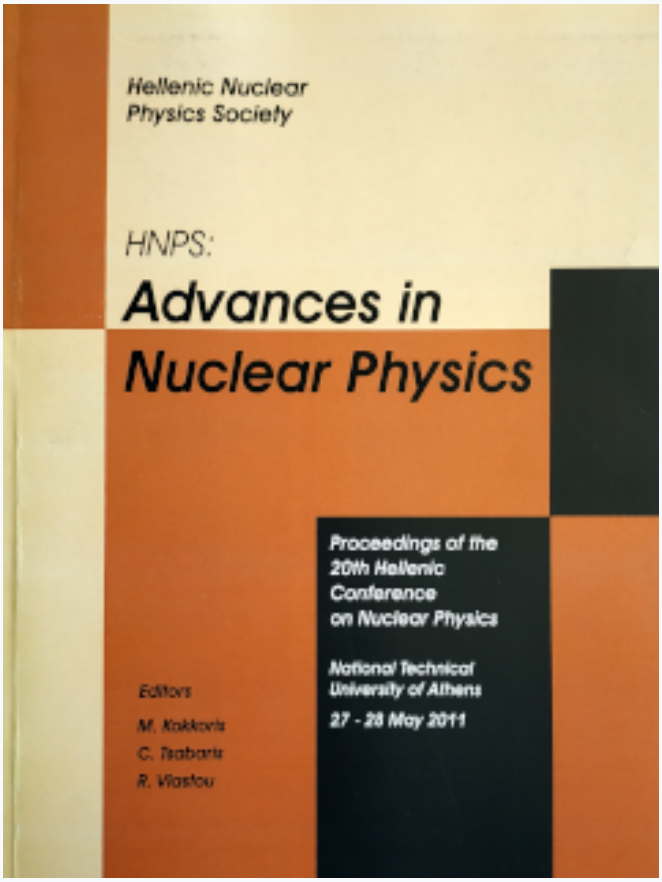

Approaching neutron-rich nuclei towards the r-process path in 86Kr-induced collisions at 15 MeV/nucleon

G. A. Souliotis

doi: 10.12681/hnps.2519

Approaching neutron-rich nuclei towards the r-process path in ^{86}Kr-induced collisions at 15 MeV/nucleon

George A. Souliotis

Laboratory of Physical Chemistry, Department of Chemistry, National and Kapodistrian University of Athens, Athens 15771, Greece

Abstract

The production cross sections of projectile-like fragments from collisions of 15 MeV/nucleon ^{86}Kr with ^{64,58}Ni and ^{124,112}Sn have been measured using a magnetic separator with emphasis on the neutron-rich isotopes. Neutron pick-up isotopes (with up to 6-8 neutrons picked-up from the target) were observed with large cross sections. The present results were also compared with our previous data of the same reactions at 25 MeV/nucleon. The data at 15 MeV/nucleon show enhanced production of neutron-rich isotopes very close to the projectile, relative to the corresponding data at 25 MeV/nucleon. The large cross sections of such reactions involving peripheral nucleon exchange, indicate that these reactions offer a novel route to access extremely neutron-rich rare isotopes towards the the astrophysical r-process path and the neutron-drip line.

1 Introduction

The exploration of the nuclear landscape towards the astrophysical r-process path and the neutron drip-line have recently received exceptional attention by the nuclear physics community (see, e.g., [1] and references therein). Intimately related to this endeavor is the efficient production of very neutron-rich nuclides which constitutes a central issue in current and future rare isotope beam facilities (see, e.g., [2–8]).

Neutron-rich nuclides are mainly produced by spallation, fission and projectile fragmentation [9]. Spallation is an important mechanism to produce rare isotopes for ISOL-type techniques [10]. Projectile fission is a prolific production approach mainly in the region of light and heavy fission fragments (see, e.g., [11] for recent efforts on ^{238}U projectile fission). Finally, projectile fragmentation offers a very successful approach to produce a broad range of exotic

nuclei at beam energies above 100 MeV/nucleon (see, e.g., [12,13] for recent work on projectile fragmentation). This approach is, nevertheless, based on the fact that optimum neutron excess in the fragments is achieved by stripping the maximum possible number of protons (and no neutrons, or a minimum possible number of neutrons).

To reach a very high neutron-excess in the products, apart from proton stripping, it may be necessary to capture neutrons from the target. Such a possibility is offered by reactions of nucleon exchange which prevail at beam energies from the Coulomb barrier [14,15] to the Fermi energy (20–40 MeV/nucleon) [16–19]. Detailed experimental data in this broad energy range are scarce at present, mostly due to the complex procedure of identification and separation [15,20,21] caused, primarily, by the wide charge state distribution of the reaction products. In multinucleon transfer and deep-inelastic reactions near the Coulomb barrier [15], the low velocities of the fragments and the wide angular and ionic charge state distributions may limit the collection efficiency for the most neutron-rich products. The reactions in the Fermi energy regime combine the advantages of both low-energy (i.e., near and above the Coulomb barrier) and high-energy (i.e., above 100 MeV/nucleon) reactions. At this energy, the synergy of both the projectile and the target enhances the N/Z of the fragments, while the fragment velocities are high enough to allow efficient in-flight collection and separation.

Our previous experimental studies of projectile fragments from the reactions of 25 MeV/nucleon ^{86}Kr on ^{64}Ni [18] and ^{124}Sn [19] indicated substantial production of neutron-rich fragments. The production mechanism was described by a deep-inelastic transfer model [23], followed by a deexcitation model [24]. In order to advance our understanding of the evolution of the reaction mechanisms and, furthermore, motivated by recent developments in several facilities that will offer either very intense primary beams [4,7,25] at this energy range or re-accelerated rare isotope beams [3,4,7,8], we undertook experimental studies at 15 MeV/nucleon presented in this contribution.

2 Outline of the experimental methods

We performed mass spectrometric measurements of production cross sections of neutron-rich projectile fragments from the reactions of a 15 MeV/nucleon ^{86}Kr beam with ^{64}Ni, ^{58}Ni and ^{124}Sn, ^{112}Sn targets. A thorough presentation of the experimental method and the results will appear in [22]. The measurements were performed around the grazing angles of the corresponding reactions at 15 MeV/nucleon (6.0^o and 9.0^o for the Kr+Ni and Kr+Sn reactions, respectively) and in a wide Bρ window (1.1–2.0 Tesla meters) that enabled efficient collection of heavy projectile residues produced in a broad range of

energy damping, from quasielastic to deep-inelastic collisions.

We briefly outline the experimental measurements below. The projectile fragments were collected and identified using the MARS recoil separator applying the techniques developed and documented in our recent articles [18–21]. The Kr beam was sent on the primary target location of MARS at an angle with respect to the optical axis of the device. After interaction with the target, the fragments traversed a PPAC at the intermediate image location (for position/Bρ measurement and START time information) and then they were focused at the end of the device passing through a second PPAC (for image size monitoring and STOP time information). Finally the fragments were collected in a 5cm×5cm ΔE–E Si detector telescope (60 μm and 1000 μm thickness). Following standard techniques of Bρ–ΔE–E–TOF (magnetic rigidity, energy-loss, residual energy and time-of-flight, respectively), the atomic number Z, the mass number A, the velocity and the ionic charge of the fragments were obtained on an event-by-event basis (see, e.g., [18]). Data were obtained in a series of Bρ settings of the spectrometer to cover the energy and charge state distributions of the fragments.

The experiment was performed in two parts. In the first part, the beam was sent at the target at an angle of 4.0^o (covering the angular range $\Delta\theta$=2.2^o–5.8^o) and in the second part at an angle of 7.4^o (covering the range $\Delta\theta$=5.6^o–9.2^o). Thus, the polar angular range $\Delta\theta$=2.2^o–9.2^o) was covered in the combined experimental results [22]. In order to obtain total cross sections from the measured yields at the above angular interval, we used a model approach as described in our previous works [18,20]. First, we performed calculations of the yields with the codes DIT [23] for the primary interaction stage and GEMINI [24] for the deexcitation stage of the reaction. We then performed filtering of the DIT/GEMINI results for the limited angular acceptance of the spectrometer and the Bρ range covered in the measurements. We used the ratio of the filtered to unfiltered simulations to correct the measured data and extract total production cross sections for each projectile-like fragment.

3 Neutron-rich rare-isotope production

In Fig. 1, we present the mass distributions of elements Z=35–30 from the present data (closed circles) of ^{86}Kr (15 MeV/nucleon) + ^{64}Ni. We also compare the present data with our previous work [18] on the same reaction at 25 MeV/nucleon (closed diamonds). In this figure we also show the cross sections that correspond to high-energy projectile fragmentation of ^{86}Kr on ^{64}Ni as predicted by the empirical parametrization EPAX [26]. We remind that, in high-energy fragmentation, nucleon-pickup products are not produced or, at best, are highly suppressed compared to lower energy peripheral collisions.

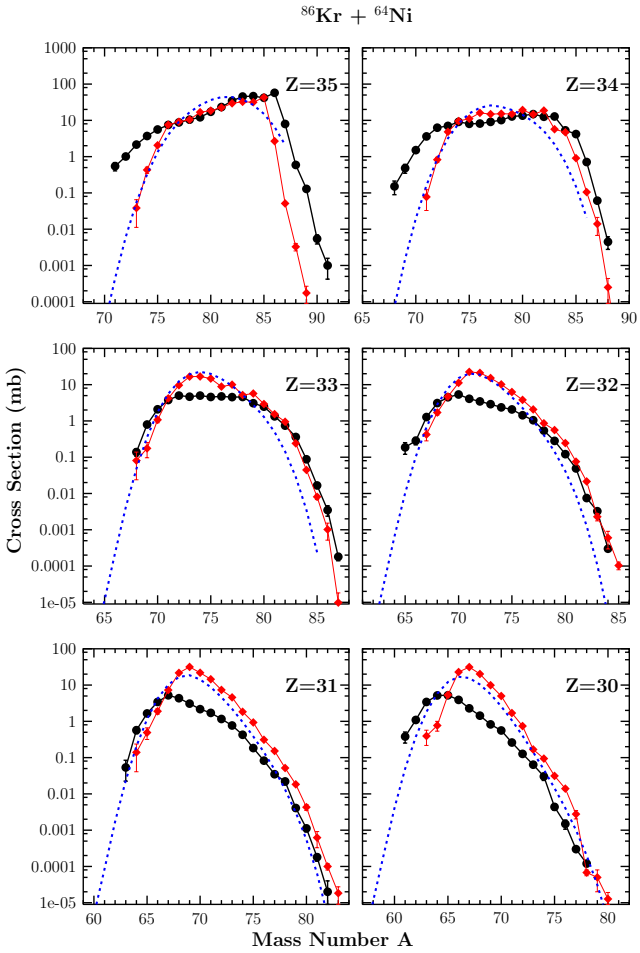

Fig. 1. Mass distributions of elements Z=35–30 from the reaction of ^{86}Kr with ^{64}Ni at 15 MeV/nucleon of this work (circles) and comparison with those of our previous work [18] at 25 MeV/nucleon (diamonds). The dotted lines are the EPAX expectations [26].

Interestingly, we observe that the reaction at 15 MeV/nucleon results in much larger cross sections for products very close to the projectile. As we see, e.g., for Br (Z=35), the most neutron-rich neutron-pickup isotopes are by a factor of 10 (or larger) more abundantly produced at 15 MeV/nucleon than at 25 MeV/nucleon. As we move further from the projectile (to lower Z elements), the cross sections of the most neutron-rich products appear to be nearly similar between the two energies. Even if a quantitative interpretation effort is the subject of upcoming work, qualitatively we can say that for the reactions at 15 MeV/nucleon, lower excitation energies of the primary fragments and larger interaction times for the most peripheral collisions may be responsible for the production and survival of residues with a large number of neutrons picked up from the target. For elements further from the projectile, the production of neutron-rich species requires a larger number of nucleons exchanged between the projectile and the target and, thus, these products possibly result from quasi-projectiles at nearly similar excitation energies, ending up with

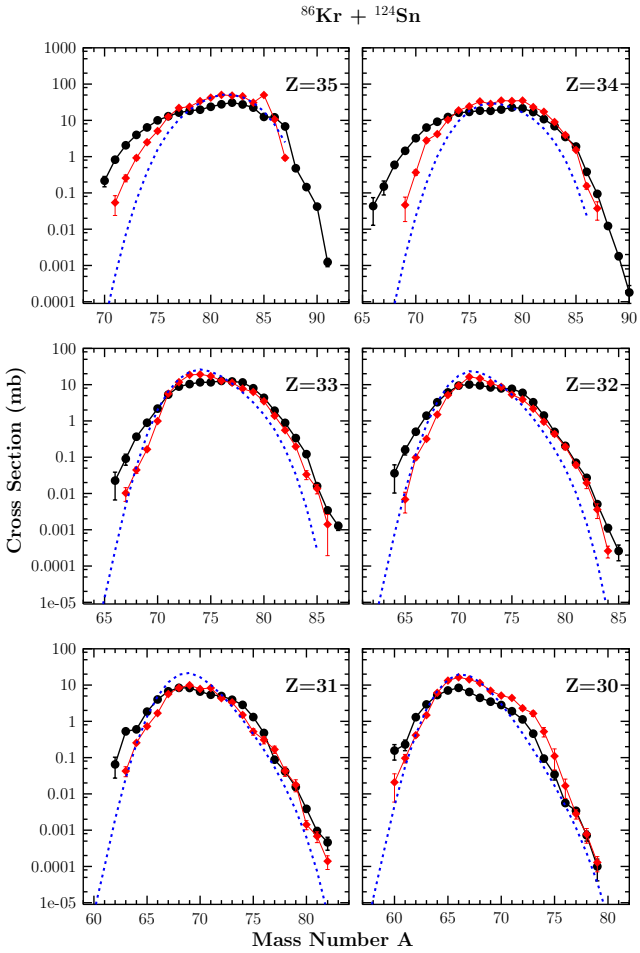

Fig. 2. Mass distributions of elements Z=35–30 from the reaction of ^{86}Kr with ^{124}Sn at 15 MeV/nucleon of this work (circles) and comparison with those of our previous work [18] at 25 MeV/nucleon (diamonds). The dotted lines are the EPAX expectations [26].

comparable cross sections at the two energies.

We also observe (Fig. 1) that for fragments further from the projectile, e.g., As (Z=33) and below, the production cross sections at the peaks of the distributions are lower at 15 MeV/nucleon as compared to those at 25 MeV/nucleon. We may qualitatively interpret this observation as an effect of the overall lower excitation energies of the quasi-projectiles obtained at 15 MeV/nucleon relative to those at 25 MeV/nucleon. The result is preferential neutron evaporation at the former energy (notice also the larger neutron-deficient tails for Z=35 and Z=34), as compared to the more extended proton and light-charged-particle evaporation (as well as sequential binary decay) leading to products at lower Z and closer to the line of β-stability at the latter energy.

Similar observations pertain to Fig. 2, in which the comparison of the 15 MeV/nucleon ^{86}Kr+^{124}Sn data to our earlier work on the same reaction at 25

MeV/nucleon [19] is presented (circles and diamonds, respectively). However, we note that the 25 MeV/nucleon data [19] do not contain the most neutron-rich products close to the projectile. Also, for fragments further from the projectile (e.g., Z=33, 32) the distributions are similar at their central and neutron-rich parts. For this system involving a heavier target, the excitation energy distributions of the primary quasi-projectiles that lead to the observed projectile-like fragments may be similar at the two energies.

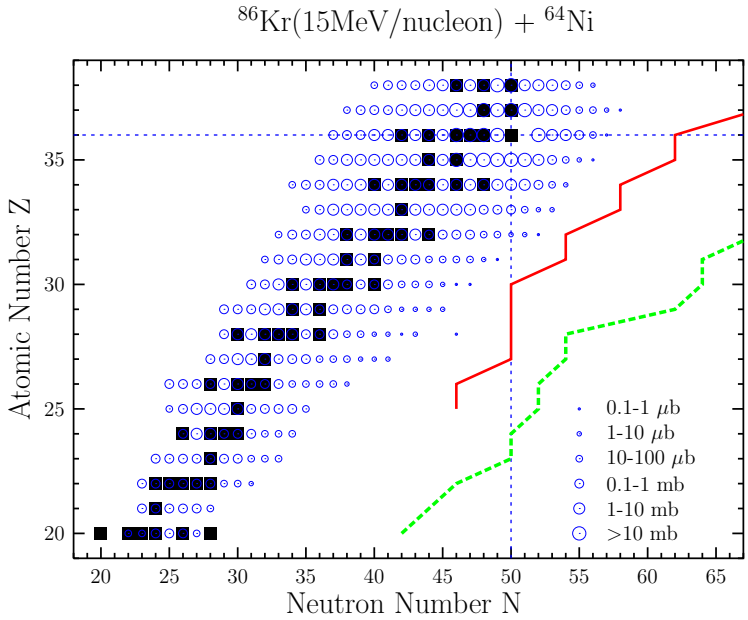

Fig. 3. Representation of the production cross sections of projectile fragments from the reaction ^{86}Kr (15 MeV/nucleon) + ^{64}Ni on the Z–N plane. The cross section ranges are shown by open circles according to the key. The closed squares show the stable isotopes. The solid line shows the astrophysical r-process path and the dashed line shows the neutron drip-line [27]. The horizontal and vertical dashed lines indicate, respectively, the proton and neutron number of the ^{86}Kr projectile.

A comprehensive presentation of the production cross sections of the projectile-like fragments from the 15 MeV/nucleon reaction ^{86}Kr + ^{64}Ni on the Z vs N plane is given in Fig. 3. In this figure, stable isotopes are represented by closed squares, whereas fragments obtained in this work are given by the open circles (with sizes corresponding to cross section ranges according to the figure key). The dashed line gives the location of the neutron drip-line and the full line indicates the expected path of the astrophysical rapid neutron-capture process (r-process), as calculated in [27]. In the figure we observe that the neutron pickup products from the ^{86}Kr projectile approach the path of the r-process near Z=32–34. We can expect that an increase of the production rates by about 10^3 (by a factor of 100–200 in beam intensity and 5–10 in target thickness) may allow accessing the r-process path nuclei in the region Z=30–36. Thus, from a practical standpoint, we may conclude that the large production cross section of neutron-rich nuclides, and, especially, the multi-neutron pick-up possibility can render these reactions a promising route to produce

extremely neutron-rich nuclides near and beyond the r-process path.

Using the present cross sections, we can make estimates of rare isotope production rates from intense beams at this energy that will become available at several facilities (e.g. [4,7]). As examples, we present in Table I the cross sections and production rates for the most neutron-rich nuclides from Kr (Z=36), Br (Z=35) and Se (Z=34). The cross sections of this work are given in the third column. The last column gives the expected rates calculated using the present cross sections and assuming a beam of 500 pnA ^{86}Kr at 15 MeV/nucleon striking a 20 mg/cm^2 ^{64}Ni target. Such yields of neutron rich isotopes will enable a variety of nuclear structure and nuclear reaction studies at this energy.

Table 1
Cross sections and rate estimates (last column) of very neutron-rich isotopes from the reaction ^{86}Kr (15 MeV/nucleon) + ^{64}Ni. For the rates, the cross section data of this work are used, and a primary beam of ^{86}Kr with intensity 500 pnA is assumed to interact with a ^{64}Ni target of 20 mg/cm^2 thickness.

Rare Isotope	Reaction Channel	Cross Section	Rate (sec^{-1})
^{90}Kr	-0p+4n	2.7 mb	1.6×10^{6}
^{91}Kr	-0p+5n	0.21 mb	1.3×10^{5}
^{92}Kr	-0p+6n	20 μb	1.2×10^{4}
^{93}Kr	-0p+7n	1.1 μb	7×10^{2}
^{87}Br	-1p+2n	8.0 mb	4.8×10^{6}
^{88}Br	-1p+3n	0.59 mb	3.5×10^{5}
^{89}Br	-1p+4n	0.13 mb	7.8×10^{4}
^{90}Br	-1p+5n	5.4 μb	3.2×10^{3}
^{91}Br	-1p+6n	1.0 μb	6×10^{2}
^{84}Se	-2p+0n	5.3 mb	3.2×10^{6}
^{85}Se	-2p+1n	4.2 mb	2.5×10^{6}
^{86}Se	-2p+2n	0.71 mb	4.2×10^{5}
^{87}Se	-2p+3n	60 μb	3.6×10^{4}
^{88}Se	-2p+4n	4.4 μb	2.6×10^{3}

Finally, another interesting possibility is the use of such reactions as a second stage in two-stage rare-isotope production schemes. For example, a beam of

^{92}Kr from an ISOL facility can be accelerated at 15 MeV/nucleon and subsequently strike a ^{64}Ni target to produce very neutron-rich nuclides that may be separated and studied in flight. To estimate the rates of such reaction products, the cross sections of this work may be used as a rough approximation. However, a quantitative prediction will be possible after obtaining an adequate theoretical description of these peripheral collisions between neutron-rich nuclei at this energy, which is one of the goals of upcoming work.

4 Summary and conclusions

In summary, the present work described the mass spectrometric measurements of the production cross sections of projectile-like fragments from the reactions of 15 MeV/nucleon ^{86}Kr with ^{64,58}Ni and ^{124,112}Sn. The measurements were performed in a wide angular range near the grazing angle of the systems. Special emphasis was given on the neutron-rich isotopes. Along with usual proton-removal products, neutron pick-up isotopes (with up to 6-8 neutrons picked-up from the target) were observed with large cross sections. The present experimental results were also compared to our previous data of the same reactions at 25 MeV/nucleon [18,19]. The data at 15 MeV/nucleon show enhanced production of neutron-rich isotopes very close to the projectile, relative to the corresponding data at 25 MeV/nucleon. This enhancement in the cross sections may be associated with very peripheral collisions and long interaction times of the neutron-rich ^{86}Kr projectile with the neutron-rich targets. Such reactions well above the Coulomb barrier, but below the Fermi energy, involving peripheral nucleon exchange, offer a new approach to access extremely neutron-rich rare isotopes towards the the r-process path and, furthermore, the neutron-drip line.

5 Acknowledgement

The author wishes to thank M. Veselsky, A.Keksis, B.C. Stein, S. Galanopoulos, M. Jandel, D.V. Shetty and S.J. Yennello for the help and support on the experimental work related to the heavy-residue measurements at 15–25 MeV/nucleon at Texas A&M. The present work was supported in part by the Department of Energy through grant No. DE-FG03-93ER40773.

References

[1] J. Äystö, W. Nazarewicz, M. Pfützner, C. Signorini, eds, Proceedings of the Fifth International Conference on Exotic Nuclei and Atomic Masses (ENAM'08), Ryn, Poland, September 7–13 (2008); Eur. Phys. J. A **42** (2009).

[2] D. F. Geesaman, C. K. Gelbke, R. V. F. Janssens, B. M. Sherrill, Ann. Rev. Nucl. Part. Sci. **56**, 53 (2006)

[3] FRIB main page: www.frib.msu.edu

[4] GANIL main page: www.ganil.fr

[5] GSI main page: www.gsi.de

[6] RIBF main page: www.rarf.riken.go.jp/Eng/facilities/RIBF.html

[7] ATLAS main page: www.phy.anl.gov/atlas/facility/index.html

[8] EURISOL main page: www.eurisol.org

[9] H. Geissel, G. Munzenberg, Ann. Rev. Nucl. Part. Sci., **45**, 163 (1995).

[10] A. Kelić, M. V. Ricciardi, K. -H. Schmidt, BgNS Transactions, **13**, 98 (2009).

[11] H. Alvarez-Pol et al., Phys. Rev. C **82**, 041602 (2010).

[12] O. B. Tarasov et al., Phys. Rev. C **80**, 034609 (2009).

[13] S. Lukyanov et al., Phys. Rev. C **80**, 014609 (2009).

[14] V. V. Volkov, Phys. Rep. **44**, 93 (1978).

[15] L. Corradi, G. Pollarolo, S. Szilner, J. Phys. G **36**, 113101 (2009).

[16] M. Veselsky, Phys. Rev. C **62**, 064613 (2000).

[17] M. Veselsky, G.A. Souliotis, Nucl.Phys. **A 765**, 252 (2006).

[18] G. A. Souliotis et al., Phys. Lett. B **543**, 163 (2002).

[19] G. A. Souliotis et al., Phys. Rev. Lett. **91**, 022701 (2003).

[20] G. A. Souliotis et al., Nucl. Instrum. Methods **B 204** 166 (2003).

[21] G. A. Souliotis et al., Nucl. Instum. Methods **B 266**, 4692 (2008).

[22] G. A. Souliotis et al., Phys. Rev. C submitted (2011).

[23] L. Tassan-Got and C. Stephan, Nucl. Phys. **A 524**, 121 (1991).

[24] R. Charity et al., Nucl. Phys. **A 483**, 391 (1988); Phys. Rev. **C 58**, 1073 (1998).

[25] Texas A&M Cyclotron Institute main page: cyclotron.tamu.edu

[26] K. Summerer, B. Blank, Phys. Rev. **C 61**, 034607 (2000).

[27] P. Moller, J.R. Nix and K.L. Kratz, At. Data Nucl. Data Tables **66**, 131 (1997).